

Evaluating the Sensitivity of Intermediate Temperature Performance Tests With Short-Term and Long-Term Laboratory Conditioning: Validation Study

January 2025

Publication No. FHWA-HRT-24-147



U.S. Department of Transportation
Federal Highway Administration

Research, Development, and Technology
Turner-Fairbank Highway Research Center
6300 Georgetown Pike McLean, VA 22101-2296

Turner-Fairbank
| Highway Research Center

FOREWORD

This report provides an independent evaluation of the capabilities of different laboratory-conducted, intermediate-temperature asphalt mixture performance tests under short- and long-term oven-aging (LTOA) conditions. An examination of test outcomes before and after extended LTOA conditioning emphasizes the responsiveness of standard laboratory performance tests and offers insights into material behavior under varied aging conditions.

The report describes the third phase of FHWA's Mixture Performance Test Comparison study, a seamless continuation of phases I and II, wherein asphalt mixtures from three different States, featuring varying nominal maximum aggregate sizes, underwent examination both before and after the application of two emerging LTOA procedures.

The advancement of balanced-mixture-design procedures requires appropriate thresholds and careful characterization of mixtures in production and service settings, as well as correlation with documented pavement performance. Included in this study is a discussion on the different percentages of reclaimed materials available in asphalt mixtures and the variety of intermediate cracking tests that introduce varying behavioral insights during a pavement's life cycle.

Findings from this study bridge an important gap between different aging practices nationwide and performance test results. This report should benefit public and private stakeholders who develop specifications or conduct research on asphalt balanced mixture design programs.

Jean A. Nehme, Ph.D., P.E.
Director, Office of Infrastructure
Research and Development

Notice

This document is disseminated under the sponsorship of the U.S. Department of Transportation (USDOT) in the interest of information exchange. The U.S. Government assumes no liability for the use of the information contained in this document.

Non-Binding Contents

Except for the statutes and regulations cited, the contents of this document do not have the force and effect of law and are not meant to bind the States or the public in any way. This document is intended only to provide information regarding existing requirements under the law or agency policies.

Quality Assurance Statement

The Federal Highway Administration (FHWA) provides high-quality information to serve Government, industry, and the public in a manner that promotes public understanding. Standards and policies are used to ensure and maximize the quality, objectivity, utility, and integrity of its information. FHWA periodically reviews quality issues and adjusts its programs and processes to ensure continuous quality improvement.

Disclaimer for Product Names and Manufacturers

The U.S. Government does not endorse products or manufacturers. Trademarks or manufacturers' names appear in this document only because they are considered essential to the objective of the document. They are included for informational purposes only and are not intended to reflect a preference, approval, or endorsement of any one product or entity.

Recommended citation: Federal Highway Administration, *Evaluating the Sensitivity of Intermediate Temperature Performance Tests With Short-Term and Long-Term Laboratory Conditioning: Validation Study* (Washington, DC: 2024) <https://doi.org/10.21949/1521783>

TECHNICAL REPORT DOCUMENTATION PAGE

1. Report No. FHWA-HRT-24-147	2. Government Accession No.	3. Recipient's Catalog No.	
4. Title and Subtitle Evaluating the Sensitivity of Intermediate Temperature Performance Tests With Short-Term and Long-Term Laboratory Conditioning: Validation Study		5. Report Date January 2025	
		6. Performing Organization Code	
7. Author(s) Varun Veginati (ORCID: 0000-0003-0875-9356), David J. Mensching, Ph.D., P.E. (ORCID: 0000-0003-2460-2586), Michael D. Elwardany, Ph.D., P.E. (ORCID: 0000-0003-4787-7478), Adrian Andriescu, Ph.D. (ORCID: 0000-0003-2548-5545), Hamzeh F. Haghshenas, Ph.D. (ORCID: 0000-0002-4234-4536) Behnam Jahangiri, Ph.D., P.E. (ORCID: 0000-0002-5345-7034)		8. Performing Organization Report No.	
9. Performing Organization Name and Address Asphalt Binder Mixture Laboratory Turner-Fairbank Highway Research Center 6300 Georgetown Pike McLean, VA 22101-2296		10. Work Unit No. (TRAIS)	
		11. Contract or Grant No. DTFH61-17-D-00017	
12. Sponsoring Agency Name and Address Office of Infrastructure Research and Development Federal Highway Administration 6300 Georgetown Pike McLean, VA 22101		13. Type of Report and Period Covered Final Report; June 2019–December 2021	
		14. Sponsoring Agency Code HRDI-10	
15. Supplementary Notes The Contracting Officer's Representative for this report was Cara Fitzgerald (HRDI-1). The Task Order Contracting Officer's Representative was David J. Mensching, Ph.D., P.E. (HRDI-10; ORCID: 0000-0003-2460-2586).			
16. Abstract Balanced mixture design (BMD) of asphalt mixtures comprises various elements that are likely to impact asphalt pavement performance. However, most BMD applications do not account for long-term aging. This gap limits the appropriateness of thresholds and BMD's potential to improve pavement performance because more additives and reclaimed materials available can behave in drastically different fashions during early, intermediate, and late stages of service. This report details the third phase of this study, in which phase I focused on the value of intermediate-temperature performance tests after short-term oven aging, which is included in current BMD frameworks, and phase II focused on highlighting the sensitivity—or lack thereof—of common laboratory mixture performance tests to long-term aging. In this study, materials from four different States are subjected to long-term oven-aging (LTOA) conditions. The materials are plant-mixed, laboratory-compacted specimens from Florida, Montana, Ohio, and Vermont, with different nominal maximum aggregate sizes and reclaimed asphalt pavement (RAP) percentages. The indirect tensile cracking test, Illinois Flexibility Index Test (I-FIT), asphalt mixture performance tester cyclic fatigue test, and dynamic modulus test were used. Two LTOA methods for intermediate cracking tests were selected based on mixture location. The main objective of this report is to evaluate the impacts of LTOA on mixture performance. The results were analyzed to compare the differences between the cracking tests, which showed a reduction in mixture cracking indexes when LTOA is incorporated. The pattern of the indexes from this validation phase (phase III) matched well with those from phase II. The I-FIT showed more variability than the two other cracking test methods. The findings in this report illustrate that long-term aging is critical for a comprehensive BMD framework. Thus, more efforts are needed to revise some of the testing protocols, indexes, and thresholds before formulating BMD specifications with LTOA conditioning.			
17. Key Words Aging, reclaimed asphalt pavement, RAP, reclaimed asphalt shingle, RAS, balanced-mixture design, performance testing, cracking, asphalt mixture performance, cyclic fatigue		18. Distribution Statement No restrictions. This document is available to the public through the National Technical Information Service, Springfield, VA 22161. https://www.ntis.gov	
19. Security Classif. (of this report) Unclassified	20. Security Classif. (of this page) Unclassified	21. No. of Pages 44	22. Price

Form DOT F 1700.7 (8-72)

Reproduction of completed page authorized.

SI* (MODERN METRIC) CONVERSION FACTORS				
APPROXIMATE CONVERSIONS TO SI UNITS				
Symbol	When You Know	Multiply By	To Find	Symbol
LENGTH				
in	inches	25.4	millimeters	mm
ft	feet	0.305	meters	m
yd	yards	0.914	meters	m
mi	miles	1.61	kilometers	km
AREA				
in ²	square inches	645.2	square millimeters	mm ²
ft ²	square feet	0.093	square meters	m ²
yd ²	square yard	0.836	square meters	m ²
ac	acres	0.405	hectares	ha
mi ²	square miles	2.59	square kilometers	km ²
VOLUME				
fl oz	fluid ounces	29.57	milliliters	mL
gal	gallons	3.785	liters	L
ft ³	cubic feet	0.028	cubic meters	m ³
yd ³	cubic yards	0.765	cubic meters	m ³
NOTE: volumes greater than 1,000 L shall be shown in m ³				
MASS				
oz	ounces	28.35	grams	g
lb	pounds	0.454	kilograms	kg
T	short tons (2,000 lb)	0.907	megagrams (or "metric ton")	Mg (or "t")
TEMPERATURE (exact degrees)				
°F	Fahrenheit	5 (F-32)/9 or (F-32)/1.8	Celsius	°C
ILLUMINATION				
fc	foot-candles	10.76	lux	lx
fl	foot-Lamberts	3.426	candela/m ²	cd/m ²
FORCE and PRESSURE or STRESS				
lbf	poundforce	4.45	newtons	N
lbf/in ²	poundforce per square inch	6.89	kilopascals	kPa
APPROXIMATE CONVERSIONS FROM SI UNITS				
Symbol	When You Know	Multiply By	To Find	Symbol
LENGTH				
mm	millimeters	0.039	inches	in
m	meters	3.28	feet	ft
m	meters	1.09	yards	yd
km	kilometers	0.621	miles	mi
AREA				
mm ²	square millimeters	0.0016	square inches	in ²
m ²	square meters	10.764	square feet	ft ²
m ²	square meters	1.195	square yards	yd ²
ha	hectares	2.47	acres	ac
km ²	square kilometers	0.386	square miles	mi ²
VOLUME				
mL	milliliters	0.034	fluid ounces	fl oz
L	liters	0.264	gallons	gal
m ³	cubic meters	35.314	cubic feet	ft ³
m ³	cubic meters	1.307	cubic yards	yd ³
MASS				
g	grams	0.035	ounces	oz
kg	kilograms	2.202	pounds	lb
Mg (or "t")	megagrams (or "metric ton")	1.103	short tons (2,000 lb)	T
TEMPERATURE (exact degrees)				
°C	Celsius	1.8C+32	Fahrenheit	°F
ILLUMINATION				
lx	lux	0.0929	foot-candles	fc
cd/m ²	candela/m ²	0.2919	foot-Lamberts	fl
FORCE and PRESSURE or STRESS				
N	newtons	2.225	poundforce	lbf
kPa	kilopascals	0.145	poundforce per square inch	lbf/in ²

*SI is the symbol for International System of Units. Appropriate rounding should be made to comply with Section 4 of ASTM E380.
(Revised March 2003)

TABLE OF CONTENTS

CHAPTER 1. INTRODUCTION	1
CHAPTER 2. OBJECTIVE AND SCOPE	3
CHAPTER 3. MATERIALS AND METHODS.....	5
Materials	5
Selected Laboratory Aging Duration Maps	6
METHODS: Asphalt Mixture Testing Procedures	7
IDEAL-CT	7
I-FIT	8
AMPT Dynamic Modulus Test.....	9
AMPT Cyclic Fatigue Test	10
Asphalt Binder Test Methods	11
CHAPTER 4. RESULTS AND DISCUSSION.....	17
Phase III Asphalt Mixture Results Discussion	17
IDEAL-CT Results	17
<i>FI</i> Results	18
<i>S_{app}</i> Results.....	19
<i>E[*]/Sin(δ)</i> Results	21
Mapping Linear Viscoelastic Aging Index Against Cracking Tests for STOA Versus LTOA.	21
Phase III Binder Results Discussion.....	25
Binder Rheology Correlations	26
CHAPTER 5. CONCLUSIONS.....	29
ACKNOWLEDGMENTS	31
REFERENCES.....	33

LIST OF FIGURES

Figure 1. Map. Required oven-aging duration at 95 °C (203 °F). ⁽⁵⁾	7
Figure 2. Photo. Test setup for IDEAL-CT.	8
Figure 3. Photo. I-FIT sample in AMPT	9
Figure 4. Graph. Separation of data in mixture Black Space when moving toward prephase angle peak. ⁽³⁰⁾	10
Figure 5. Photos. Automated binder extraction and recovery instrument.	12
Figure 6. Photo. DSR.	13
Figure 7. Photo. Computer-controlled Duclilometer.	14
Figure 8. Photo. Image of the ductility instrument loading area during a DENT test.	15
Figure 9. Photo. A Fourier transform infrared spectrometer with attenuated total reflectance capability.	16
Figure 10. Graph. CT_{Index} at STOA and LTOA levels for all mixtures at testing temperature.	18
Figure 11. Graph. FI at STOA and LTOA levels for all mixtures at testing temperature.	19
Figure 12. Graph. S_{app} at STOA and LTOA levels for all mixtures at individual testing temperature.	20
Figure 13. Graph. S_{app} at STOA and LTOA levels for all mixtures at 18 °C (64.4 °F).	20
Figure 14. Graph. Log $E^*/\sin(\delta)$ at STOA and LTOA levels for all mixtures at testing temperature.	21
Figure 15. Graphs. Relationship between cracking test indexes and $ E^* /\sin(\delta)$ at STOA and 135 °C (275 °F) LTOA.	22
Figure 16. Graphs. Relationship between cracking test indexes and $ E^* /\sin(\delta)$ at STOA and 95 °C (203 °F) LTOA.	23
Figure 17. Graph. CTOD at STOA and LTOA levels for all mixtures.	26
Figure 18. Graph. Relationship between cracking test indexes and $ G^* /\sin(\delta)$ at STOA and 135 °C (275 °F) LTOA.	27
Figure 19. Graphs. Relationship between cracking test indexes and $ G^* /\sin(\delta)$ at STOA and 95 °C (203 °F) LTOA.	28

LIST OF TABLES

Table 1. Featured mixtures from the four different States.....	5
Table 2. Selected LTOA temperature for mixtures.	6
Table 3. Summary of index values from the four States at different aging levels.....	24
Table 4. Summary of COV (in percent) of index values from the four different States at different aging levels.....	25

LIST OF ABBREVIATIONS

AASHTO	American Association of State Highway and Transportation Officials
AMPT	asphalt mixture performance tester
ANOVA	analysis of variance
BMD	balanced mixture design
COV	coefficient of variation
CT _{Index}	cracking tolerance index
CTOD	critical-tip-opening displacement
DSR	dynamic shear rheometer
FHWA	Federal Highway Administration
FI	flexibility index
GR	Glover–Rowe
IDEAL-CT	indirect tensile asphalt cracking test
I-FIT	Illinois flexibility index test
LTOA	long-term oven aging
NCAT	National Center for Asphalt Technology
NCHRP	National Cooperative Highway Research Program
NMAS	nominal maximum aggregate size
RAP	reclaimed asphalt pavement
RAS	reclaimed asphalt shingle
STOA	short-term oven aging

CHAPTER 1. INTRODUCTION

Fatigue cracking has always been a challenging issue with regard to asphalt pavements. It is one of the primary distresses due to repeated loading on asphalt pavements. Aging in asphalt pavements has been recognized and studied for almost a century. Hubbard and Reeve published the first results of a study that examined the effects of a year of outdoor weathering on the physical (weight, hardness, etc.) and chemical (solubility) properties of paving-grade asphalt cements.⁽¹⁾ Subsequent studies confirmed Hubbard and Reeve's basic finding that oxidation, and not volatilization alone, is responsible for changes in asphalt properties that occur due to exposure.⁽²⁻⁴⁾ Further oxidative aging of asphalt is a long-held area of both curiosity and concern among materials engineers. As asphalt materials age, the cracking susceptibility of the mixtures changes during the course of time. More recently, several researchers have proposed that asphalt mixtures be long-term aged in the loose state. (See references 5 through 9.) The rate of oxidation increases at higher temperatures, and thus, many researchers have proposed loose-mix aging at 135 °C (275 °F) as an efficient alternative to the American Association of State Highway and Transportation Officials (AASHTO) R 30 aging protocol.^(8,10) Researchers have also mentioned that chemical changes that occur when loose mixtures are aged at 135 °C (275 °F) can lead to significantly different cracking performance results compared with materials testing and pavement simulations for aging at 95 °C (203 °F).⁽⁵⁾ Thus, the National Cooperative Highway Research Program (NCHRP) has conducted research to investigate loose-mixture aging versus compacted-specimen aging, oven aging versus pressure aging, and 95 °C (203 °F) aging temperature versus 135 °C (275 °F).⁽¹¹⁾ Based on the results, researchers have proposed the conditioning of loose mixture in an oven at 95 °C (203 °F) as the long-term aging procedure for the fabrication of asphalt mixture performance test specimens.⁽¹¹⁾

The Federal Highway Administration (FHWA) has started a three-phase project entitled Mixture Performance Test Comparison Study:

- The first phase focused on the value of intermediate-temperature performance tests after short-term oven aging (STOA), which is included in current balanced mixture design (BMD) frameworks.
- The second phase focused on comparing aging approaches—particularly whether equivalence between long-term-aging procedures exists—and on highlighting the sensitivity—or lack thereof—of common laboratory mixture performance tests.
- This report presents the results of the third phase of the project. Phase III is intended to investigate the impacts of long-term aging on mixture performance, and plant-mixed, laboratory-compacted mixtures from various States will be subjected to long-term oven aging (LTOA).

Three commonly discussed cracking performance tests from phases I and II were applied in phase III: the Asphalt Mixture Performance Tester (AMPT) cyclic fatigue test, the Illinois Flexibility Index Test (I-FIT), and the indirect tensile asphalt cracking test (IDEAL-CT). The tests were selected after a review of the results from phase I and phase II and technical input from the stakeholders.

CHAPTER 2. OBJECTIVE AND SCOPE

The objective of this study is to investigate the impacts of long-term aging on mixture performance. Loose mixtures from four different States were subjected to LTOA to understand the diversity of the mixtures, to determine stiffness dependency of the test methods, and to link binder and mixture properties that were not parts of phase I and phase II.

The objective of the parent study, entitled Mixture Performance Test Comparison Study, is to provide information for the community with regard to the intermediate-temperature performance tests and changes noticed due to the incorporation of laboratory aging. To reduce variability that might result from multiple operators, one technician prepared all test specimens, and a separate technician tested all specimens. Each technician has approximately 35 yr of experience in asphalt materials research laboratories.

CHAPTER 3. MATERIALS AND METHODS

MATERIALS

The materials included in this report are from Florida, Montana, Ohio, and Vermont and represent different nominal maximum aggregate sizes (NMASs) and different reclaimed asphalt pavement/reclaimed asphalt shingle (RAP/RAS) percentages, as shown in table 1. The naming of each mixture is labeled (State)(NMAS)(percent RAP). For example, FL12.5R00 reads as the mixture from Florida, with a 12.5-mm (0.5-inch) NMAS and 0 percent RAP.

Table 1. Featured mixtures from the four different States.

State	Mixture	Percent RBR	VMA	VFA	Percent AC	G_{mm}	G_{mb}	G_{sb}
Florida	FL12.5R00	0 RAP	18.0	62.1	5.0	2.541	2.359	2.734
Montana	MT9.5R00	0 RAP	18.7	63.1	5.9	2.402	2.320	2.588
Montana	MT19R00	0 RAP	16.1	58.7	5.0	2.455	2.367	2.606
Ohio	OH9.5R20	20 RAP	20.6	66.0	6.3	2.423	2.338	2.614
Ohio	OH12.5R15	15 RAP	19.1	63.6	5.9	2.475	2.376	2.640
Ohio	OH19R18	18 RAP	16.2	56.9	5.3	2.452	2.354	2.616
Vermont	VT12.5R00	0 RAP	19.4	62.2	5.8	2.478	2.379	2.684

AC = asphalt content; G_{mb} = bulk specific gravity of asphalt mixture; G_{mm} = maximum theoretical specific gravity; G_{sb} = bulk specific gravity of aggregate; RBR = reclaimed binder ratio; VFA = voids filled with asphalt; VMA = voids in mineral aggregate.

This study used one STOA procedure (reheated to compaction temperature) and two loose LTOA procedures after gathering stakeholder input. The first approach is from NCHRP project 09-54, which relies on oven conditioning at 95 °C (203 °F). Researchers generated a series of maps detailing LTOA duration to simulate conditions across the United States for various target service times and various depths from the surface. The first LTOA duration corresponded to 8 yr of field aging at a depth of 20 mm (0.8 inch) below the surface to represent the state of a 50-mm (2-inch) surface lift.⁽¹²⁾ Conversely, a higher temperature, shorter duration aging technique was also used. The approach was generated through work at the National Center for Asphalt Technology (NCAT), with an oven conditioning temperature of 135 °C (275 °F) and a duration of 8 h.⁽¹³⁾ The premise behind the method is that different cumulative degree-days would be simulated by the oven conditioning based on field location. The two LTOA temperatures and the duration for individual mixtures are shown in table 2.

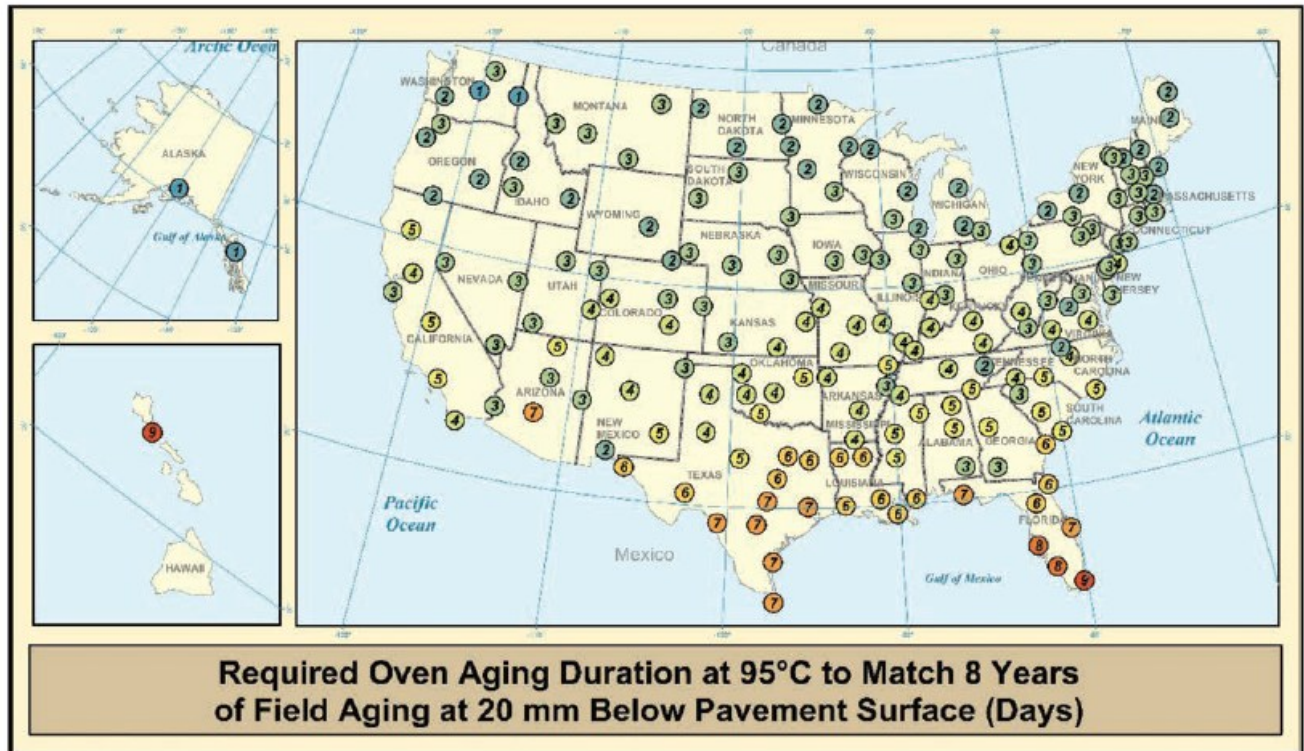
Table 2. Selected LTOA temperature for mixtures.

State	Mixture	95 °C (203 °F)	135 °C (275 °F)
Florida	FL12.5R00	7 d	8 h
Montana	MT9.5R00	3 d	8 h
Montana	MT19R00	3 d	8 h
Ohio	OH9.5R20	4 d	8 h
Ohio	OH12.5R15	4 d	8 h
Ohio	OH19R18	4 d	8 h
Vermont	VT12.5R00	3 d	8 h

As mentioned, the researchers conducted four different mixture performance tests on the aged materials. In all cases, the target air void level was 7 ± 0.5 percent. Dynamic modulus testing was conducted on 38-mm-(1.5-inch)diameter by 110-mm-(4.3-inch)height specimens in general accordance with AASHTO TP 132.⁽¹⁴⁾ Deviations from AASHTO TP 132 are related exclusively to the temperature and frequency combinations and a microstrain target of 100 that was used. Testing was conducted in an AMPT at 4.4, 21.1, 37.8, and 45 °C (40, 70, 100, 113 °F) at frequencies of 25, 10, 5, 1, 0.5, and 0.1 Hz.

SELECTED LABORATORY AGING DURATION MAPS

The aging duration for each of the selected mixtures from four different States was selected based on a mixture's location and climate. According to a climate aging index, as reported in NCHRP report 871, loose-mixture aging durations at 95 °C (203 °F) that are required to match 8 yr of field aging at a depth of 20 mm (0.8 inch) below the surface are shown in figure 1.⁽⁵⁾ A depth of 20 mm (0.8 inch) represents a reasonable depth for the evaluation of surface-layer asphalt mixtures because a depth of 20 mm (0.8 inch) better reflects the bulk behavior of the top 50-mm (2-inch) layer of the pavement structure. Conversely, a higher-temperature, shorter-duration aging technique was also used in this phase of the project. The approach was generated through work at NCAT, with an aging temperature of 135 °C (275 °F) and a duration of 8 h.⁽¹³⁾ The premise behind this method is that different cumulative degree-days will be simulated by the oven aging condition based on field location, but from a kinetics modeling perspective, these aging levels are not equal.



© 2018 National Academies of Science, Engineering, and Medicine.

Figure 1. Map. Required oven-aging duration at 95 °C (203 °F).⁽⁵⁾

METHODS: ASPHALT MIXTURE TESTING PROCEDURES

This section describes each of the four test procedures. The testing was conducted in accordance with relevant methods and guidelines. All of the tests hold AASHTO- or ASTM-approved status in accordance with either provisional or permanent methods. Each test has its own index or indexes, which are generated from measured raw data and provide options to institute pass/fail criteria for asphalt mixture design and, eventually, acceptance. This section highlights all of the indexes for the aforementioned test methods. The three cracking tests described emerged as results of research by Golalipour, Veginati, and Mensching as well as technical input from stakeholders.⁽¹⁵⁾

IDEAL-CT

Texas Transportation Institute researchers Zhou et al. developed IDEAL-CT for asphalt mixtures.⁽¹⁶⁾ The testing used a universal servohydraulic loading machine shown in figure 2 and was performed in accordance with ASTM D8225 on specimens with 62-mm (2.5-inch) thicknesses at 25 °C (77 °F) with an actuator displacement rate of 50 mm/min (2 inches/min).⁽¹⁷⁾ The index generated by this test is called the cracking tolerance index (CT_{Index}). The index is calculated from failure energy, the postpeak slope of the load displacement curve, and deformation tolerance at 75 percent of peak load. The $|m_{75}|$ term is expressed as the slope from strain tolerance at 85 percent of peak load downward to strain tolerance at 65 percent of peak load. The PPP₇₅ term can also be expressed as deformation at 75 percent of peak load (l_{75}) divided by specimen diameter (D). The equation without thickness correction is provided in equation 1. Repeatability for this test has been documented in Zhou et al. as acceptable

with a coefficient of variation (COV) of less than 25 percent.⁽¹⁶⁾ A higher CT_{Index} value represents higher cracking resistance of asphalt mixtures.



Source: FHWA.

Figure 2. Photo. Test setup for IDEAL-CT.

$$CT_{Index} = \frac{G_f}{|m_{75}|} \cdot \left(\frac{l_{75}}{D} \right) \quad (1)$$

Where:

G_f = the failure energy.

$|m_{75}|$ = the slope from the strain tolerance at 85 percent of the peak load downward to the strain tolerance at 65 percent of the peak load.

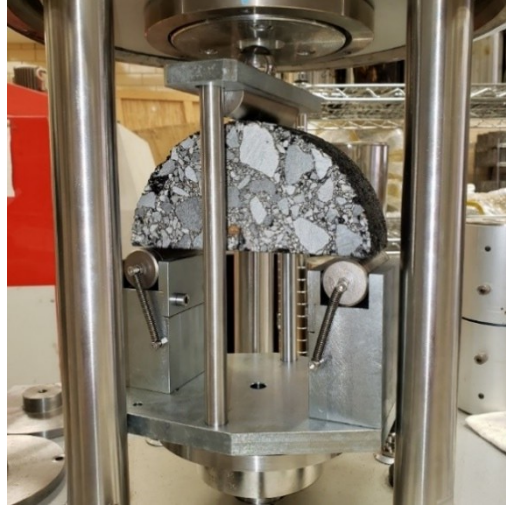
l_{75} = displacement at 75 percent of the peak load.

D = the specimen diameter.

CT_{Index} value did not exhibit sustained significant difference across a set of three RAP/RAS mixtures and one virgin mixture in research conducted by Bahia et al.⁽¹⁸⁾ Results from phase II of FHWA's research project showed that STOA has a higher cracking resistance index compared with LTOA at 95 °C (203 °F) and 135 °C (275 °F).⁽¹⁹⁾

I-FIT

I-FIT was developed at the Illinois Center for Transportation in collaboration with the Illinois Department of Transportation to assess the cracking resistance of asphalt mixtures by means of the flexibility index (FI), which was first introduced by Al-Qadi et al.^(20,21) FI is the index value generated from I-FIT. I-FIT was conducted in accordance with AASHTO T 393, which calls for a 50-mm-thick (2-inch-thick) semicircular specimen tested at 25 °C (77 °F) and a load-line displacement rate of 50 mm/min (2 inches/min).⁽²²⁾ Testing was executed in an AMPT and the sample test setup is shown in figure 3. This test uses the fracture energy, G_f (area under load-load line displacement curve divided by ligament area) in combination with the slope of the inflection point of the postpeak portion of the load-displacement curve ($|m|$). Equation 2 calculates the FI .^(20,21) The higher the FI value, the higher the crack resistance index of the asphalt mixtures.



Source: FHWA.

Figure 3. Photo. I-FIT sample in AMPT.

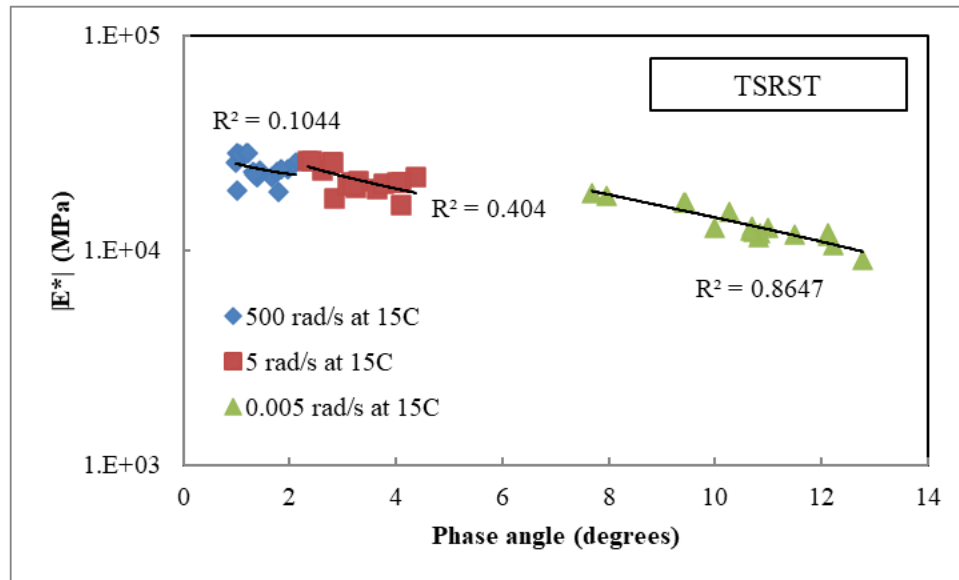
$$FI = \frac{G_f}{|m|} \cdot 0.01 \quad (2)$$

Results from NCHRP project 09-58 showed that FI decreased by 50 percent or more in most test cases in a comparison of STOA (2 h, 135 °C (275 °F)) and LTOA (5 d, 85 °C (185 °F)) on compacted specimens.⁽²³⁾ Research by Ling et al. showed strong FI sensitivity in a comparison of 4 h and 12 h of aging at 135 °C (275 °F) in a loose-mixture state.⁽²⁴⁾ Materials in the Ling et al. study included multiple intended traffic levels, aggregate sources, filler contents, and asphalt contents. Results from phase II of FHWA's research project showed that STOA has a higher cracking resistance index compared with LTOA at 95 °C (203 °F) and 135 °C (275 °F).⁽¹⁹⁾

AMPT Dynamic Modulus Test

$|E^*|$ is a fundamental property that defines the strain response characteristics of asphalt concrete mixtures as a function of loading rate and temperature, which can be achieved by running a dynamic modulus test that uses AMPT as recommended by NCHRP Project 9-19 and developed in NCHRP Project 9-29.^(25,26) $|E^*|$ testing was performed according to AASHTO TP 132 (38-mm-diameter (1.5-inch) test specimens).⁽¹⁴⁾ Specimens were cored and cut from gyratory-compacted samples. Additionally, some research has been conducted to evaluate $|E^*|$ and mixture phase angle δ , in degrees, as performance indexes—particularly as it relates to cracking resistance.⁽²⁸⁾ The incorporation of linear viscoelastic properties offers the potential to understand stress relaxation, which has an important influence on cracking susceptibility, where less stress relaxation implies high cracking susceptibility.

Work at the University of New Hampshire extended the Glover–Rowe (G_R) parameter for binders into a Black Space representation of mixtures to assess low-temperature cracking resistance.^(29,30) The G_R parameter defines a point within a Black Space plot of G^* versus phase angle. In Mensching et al. (2015), the foundation was laid to focus a rheological parameter on a temperature-frequency combination in the area of the prepeak inflection point in mixture Black Space, as illustrated in figure 4; the details were explained in the Rodeo phases I and II report.^(29,15,19)



© 2016 Association of Asphalt Paving Technologists.

Figure 4. Graph. Separation of data in mixture Black Space when moving toward prephase angle peak.⁽³⁰⁾

Mensching et al. (2016) confirms limitations of $|E^*| \cdot \sin(\delta)$ —specifically to capture cracking performance in the field.⁽²⁹⁾ These findings leave open the possibility that indexes from dynamic modulus testing that capture $|E^*|$ and δ may possess interchangeability. However, capabilities with respect to field performance correlation may be limited.

AMPT Cyclic Fatigue Test

The AMPT cyclic fatigue test is one of the fatigue cracking tests that has recently received significant attention in the pavement community. This test uses viscoelastic continuum damage principles to characterize a material's fatigue resistance and derive an index parameter. The test is intended to represent the impacts of both stiffness and toughness on mixture performance.^(31,32) Apparent damage capacity, or S_{app} , is the cyclic fatigue cracking test index used in this study. The AMPT cyclic fatigue testing was executed in accordance with AASHTO T 411, which uses the 38-mm-diameter (1.5-inch) and 110-mm-height (4.3-inch) cylindrical specimen geometry.⁽³³⁾ The tests were run in a pull-pull actuator displacement-controlled fashion at 18 °C (64.4 °F) and a 10-Hz loading rate.⁽³³⁾ Three test specimens at different on-specimen strain targets were used for each mixture. To obtain S_{app} , users have to conduct cyclic fatigue tests—to learn the initiation and progression of damage—and dynamic modulus tests to capture the linear viscoelastic response. Coupling the two tests allows for the calculation of S_{app} , as shown in equation 3, as well as inputs for structural response modeling (out of the scope of this effort). A higher index should translate to greater cracking resistance of the mixture.

$$S_{app} = 1000^{\frac{\alpha}{2}-1} \left(\frac{a_T^{\frac{1}{\alpha+1}} \left(\frac{D^R}{C_{11}} \right)^{\frac{1}{C_{12}}}}{|E^*|^{\frac{\alpha}{4}}} \right) \quad (3)$$

Where:

S_{app} = apparent damage capacity.

α = material constant derived from slope of relaxation modulus master curve in log-log scale.

a_T = time-temperature shift factor from dynamic modulus master curve.

D^R = average reduction in pseudostiffness per cycle.

C_{11}, C_{12} = damage characteristic curve fit coefficients.

$|E^*|$ = dynamic modulus at the reference temperature and 10 Hz, kPa.

The S_{app} index is sensitive to changes in loose-mixture aging.^(31,34,35) Phase II results from FHWA's study show that STOA has a higher crack resistance index compared with LTOA at 95 °C (203 °F) and 135 °C (275 °F).⁽¹⁹⁾

ASPHALT BINDER TEST METHODS

The binders from each of the seven mixtures used in the study were recovered from reheated materials and LTOA materials. LTOA for the mixture used aging temperatures of 95 °C (203 °F) and 135 °C (275 °F) (table 2). A total of 21 recovered binders were extracted in enough quantities to perform a series of rheological and failure tests at intermediate temperatures. No additional binder aging using the rolling thin-film oven and pressure-aging vessel was performed on the recovered materials. The asphalt binders were extracted in accordance with ASTM D8159 by using trichloroethylene and were recovered per ASTM D5404.^(36,37) The recovery was carried out at 135 °C (275 °F). The last 3 h of recovery were performed under a 500-mm-(19.7-inch) Hg vacuum to remove all traces of solvent. About 3.5 kg (7.7 lb) of a mixture produced about 150 grams (0.3 lb) of the recovered binder. Figure 5-A represents the automated extraction instrument, and figure 5-B represents the recovery installation.



A. Automated binder extraction instrument.



All images source: FHWA.

B. Binder recovery installation.

Figure 5. Photos. Automated binder extraction and recovery instrument.

A dynamic shear rheometer (DSR) (figure 6) characterized the rheological behavior of recovered asphalt binders per AASTHO T 315.⁽³⁸⁾ The DSR measured the viscous and elastic properties of a thin asphalt binder sample placed between an oscillating and a fixed plate.



Source: FHWA.

Figure 6. Photo. DSR.

The relationship between the applied stress and the resulting strain in the DSR provides the information necessary to calculate two important asphalt binder properties: the complex shear modulus ($|G^*|$) and the phase angle (δ). $|G^*|$ is the ratio of maximum shear stress to maximum shear strain. The time lag between the applied stress and the resulting strain is the phase angle (δ). Data was generated from frequency sweeps of 0.1–100 rad/s at different temperatures: 4, 16, 28, 40, and 52 °C (39, 60.8, 82.4, 104, and 125.6 °F). The data produced a master curve using both the principle of time–temperature superposition and the Christensen–Anderson–Marasteanu model at the reference temperature of 20 °C (68 °F).⁽³⁹⁾ The master-curves-shifted data were then used for calculating the GR parameter at 15 °C (59 °F) and 0.005 rad/s. The GR parameter, defined by equation 4, considers binder stiffness and phase angle and offers an indication of the ability to relax stresses at intermediate temperatures.⁽⁴⁰⁾

$$GR = \frac{|G^*|(\cos \delta)^2}{\sin \delta} \quad (T=44.7^\circ\text{C}, f=10 \text{ rad/s}) \quad (4)$$

The crossover modulus (G^*_c) was obtained from the master curve data generated by the DSR. The crossover modulus is defined as the complex modulus at a phase angle of 45°.

The double-edge-notched tension (DENT) test was used in this study to characterize the fracture properties of asphalt binders at intermediate temperatures per AASHTO T 405.⁽⁴¹⁾ The DENT testing apparatus is a computer-controlled Ductilometer (figure 7). The test is performed at 25 °C (77 °F) until ductile failure is reached. During testing, the energy partition between a plastic outer zone and an autonomous inner zone that is responsible for fracture is effectively measured.



Source: FHWA.

Figure 7. Photo. Computer-controlled Ductilometer.

DENT testing is based on fundamental nonlinear fracture mechanics theory. During a DENT test, the failure process consists of a continuous flow of energy through the plastic deformation region to the failure region, with energy partitioned between a plastic “outer” zone and an autonomous “inner” zone. A progressive reduction of the energy release rate in the failure zone results as the two new surfaces of material get created. Early researchers defined the work performed to create new surfaces of material in the crack end region as essential work. The total energy of ductile failure is composed of both the essential work performed in the end region and the nonessential work performed in the screening plastic region. The essential work of fracture (W_e) is proportional to the failure area (i.e., ligament length (l) multiplied by sample thickness (B)), while the nonessential work (W_p)—the plastic work—is proportional to the volume of the plastic zone (i.e., failure area ($l \times B$) multiplied by ligament length multiplied with a factor, β). The β factor depends on the shape of the plastic zone. The mathematical expression for the total work of fracture (W_f) is given in equation 5, where w_e and w_p are the corresponding specific terms for W_e and W_p .

Finally, the total work of fracture divided by the failure area ($l \times B$) becomes the total specific work of fracture (w_f), as in equation 6.

$$W_f = W_e + W_p = lBw_e + \beta l^2 Bw_p \quad (5)$$

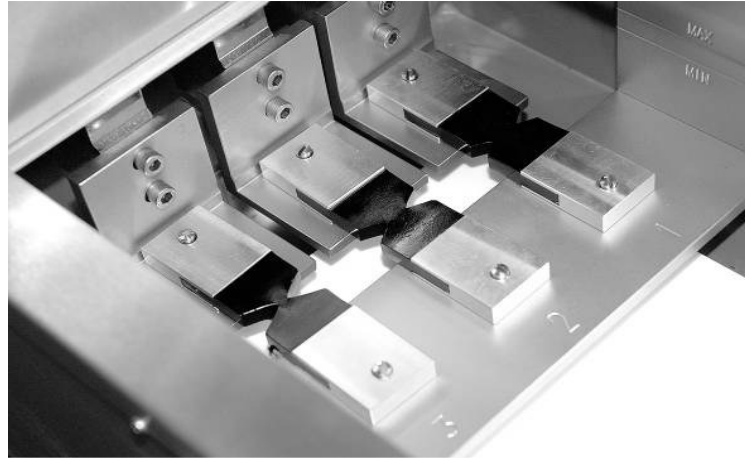
$$w_f = w_e + \beta w_p l \quad (6)$$

The plot of w_f versus l results in a straight line with an intercept equal to w_e and a slope equal to βw_p . Cotterell and Reddel observed that “the screening plastic zone vanishes for small ligaments” and determined critical-tip-opening displacement (CTOD or δ), as the ultimate elongation for zero ligament length.⁽⁴²⁾ As a result, the authors defined the value of essential work as in equation 7, where

σ represents the yield stress in tension, and σ can be approximated with the peak stress for the smallest ligament length. Finally, CTOD can be calculated as the ratio between the specific work of fracture and the peak stress for the 5-mm ligament length.

$$w_e = \delta x \sigma \quad (7)$$

The ratio of the specific essential work of failure and the yield stress of the material (approximated during the testing from the peak loads of the tested samples) can be considered the strain tolerance parameter. Figure 8 is an image of the ductility instrument during a DENT test.



Source: FHWA.

Figure 8. Photo. Image of the ductility instrument loading area during a DENT test.

Fourier transform infrared (FTIR) spectroscopy–attenuated total reflectance (ATR) was used to study oxidative-aging-related functional groups in the extracted and recovered asphalt binders. Figure 9 shows the FTIR spectrometer that generated a chemical spectrum.



Source: FHWA.

Figure 9. Photo. A Fourier transform infrared spectrometer with attenuated total reflectance capability.

ATR uses an infrared (IR) beam that is reflected off the specimen surface and then received by the detector; the measurement is then conducted by passing the IR beam through a crystal of high refractive index onto the surface of the sample with a lower index. More details regarding FTIR theoretical background can be found elsewhere.⁽⁴³⁾

Changes in the chemical structure of asphalt binders can be obtained by calculations of functional and structural indexes of specific groups. With oxidative aging, the absorbance bands representing oxygen-containing functionalities (ketones, sulfoxides, dicarboxylic anhydrides, and carboxylic acids) of asphalt increase. In this study, the scans were taken with a resolution of 4 cm^{-1} and saved as interferograms after 32 scans were performed. The interval of scanning was from 400 cm^{-1} to $4,000\text{ cm}^{-1}$. To quantify oxidation-related changes collected by means of IR, absorbance peaks were used. Then carbonyl (C=O) and sulfoxide (S=O) peaks were calculated.

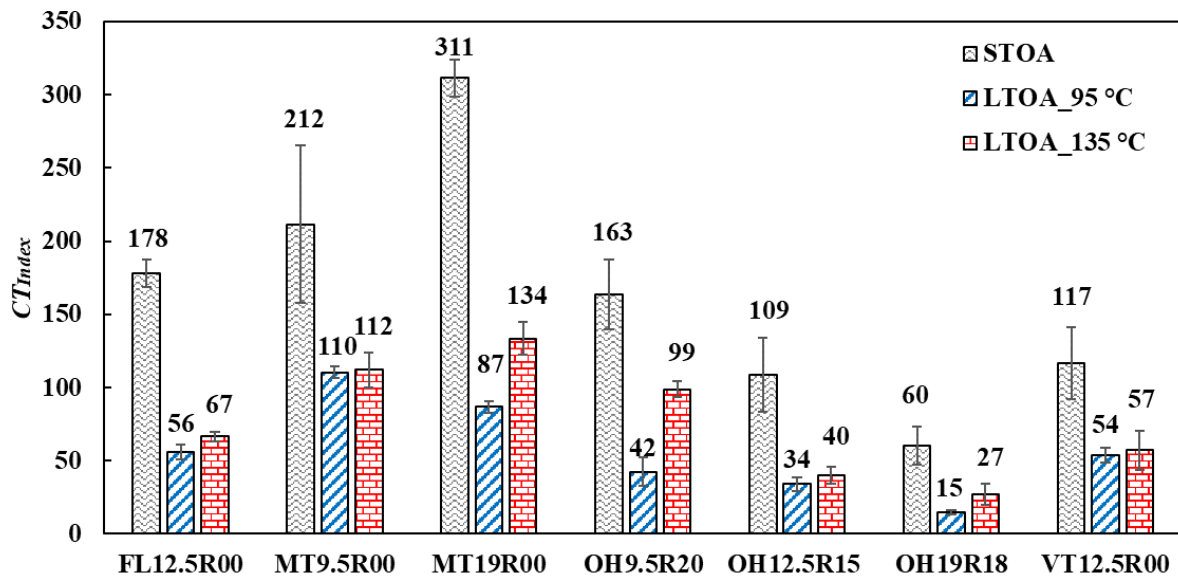
CHAPTER 4. RESULTS AND DISCUSSION

The structure of this section progresses from the results of various performance test methods at intermediate temperatures. Phase III testing isolated the difference between moderate-temperature and high-temperature LTOA procedures. Error bars in the figures represent one standard deviation of those test replicates. Each subsection shows results from a performance test method. The test results include four mixtures under STOA and LTOA conditions. The aging duration for LTOA at 95 °C (203 °F) was decided based on the project's location. Any mention of statistical significance was established through Student's *t*-test and analysis of variance (ANOVA) at an alpha (significance level) of 95 percent.

PHASE III ASPHALT MIXTURE RESULTS DISCUSSION

IDEAL-CT Results

Figure 10 shows CT_{Index} values—for all seven mixtures from four different States—that resulted from IDEAL-CT under STOA and two LTOA conditions. IDEAL-CT was conducted at 25 °C (77 °F) for all the mixtures, according to ASTM specifications. Figure 10 represents three replicates from the test at each aging level. A pattern results for all the seven mixtures: CT_{Index} value is higher at the STOA level, and the value reduced after LTOA conditioning. Overall, CT_{Index} showed promising results in differentiating STOA and LTOA conditions. Error bars in the figure represent one standard deviation of the replicates' results. In a comparison between short-term aging and long-term aging, CT_{Index} value dropped more than 50 percent from reheated to 3 d at 95 °C (203 °F) except for the Montana 9.5-mm mixture. Also, the CT_{Index} value is always higher at 135 °C (275 °F) when compared with 95 °C (203 °F). Montana mixtures showed higher crack resistance than other mixtures, which might have been due to the softer binders, as shown in $|E^*|/\sin(\delta)$ and later confirmed by binder data. Montana 19-mm shows higher crack resistance, and Ohio 19-mm shows lower crack resistance. ANOVA shows a statistically significant difference between STOA and LTOA, but not between the two LTOA methods.



Source: FHWA.

Figure 10. Graph. CT_{Index} at STOA and LTOA levels for all mixtures at testing temperature.

FI Results

Figure 11 shows *FI* values for all seven mixtures from four different States under STOA and LTOA conditions. I-FIT was conducted at 25 °C (77 °F) for all mixtures and according to AASHTO specifications. Figure 11 represents the average of three replicates from the test at each aging level and shows that *FI* value is higher under STOA condition compared with after LTOA conditioning, which is the same trend observed with IDEAL-CT results. Overall, I-FIT also showed promising results in the differentiation of STOA and LTOA. Error bars in the figure represent one standard deviation. Montana mixtures' I-FIT results displayed higher variability. When compared between STOA and LTOA, the *FI* value dropped more than 50 percent from reheated to 3 d at 95 °C (203 °F) except for Montana 19-mm and Vermont 12.5-mm mixtures. Also, the *FI* value is higher at 135 °C (275 °F) when compared with 95 °C (203 °F)—except for Ohio 19-mm and Vermont 12.5-mm mixtures. For the Ohio 19-mm mixture, the *FI* value shows similar values when comparing the two LTOA methods. Montana mixtures showed higher crack resistance compared with the other mixtures. Montana 9.5-mm shows higher crack resistance, and Ohio 19-mm shows lower crack resistance. ANOVA shows a statistically significant difference between STOA and LTOA but not between the two LTOA methods.

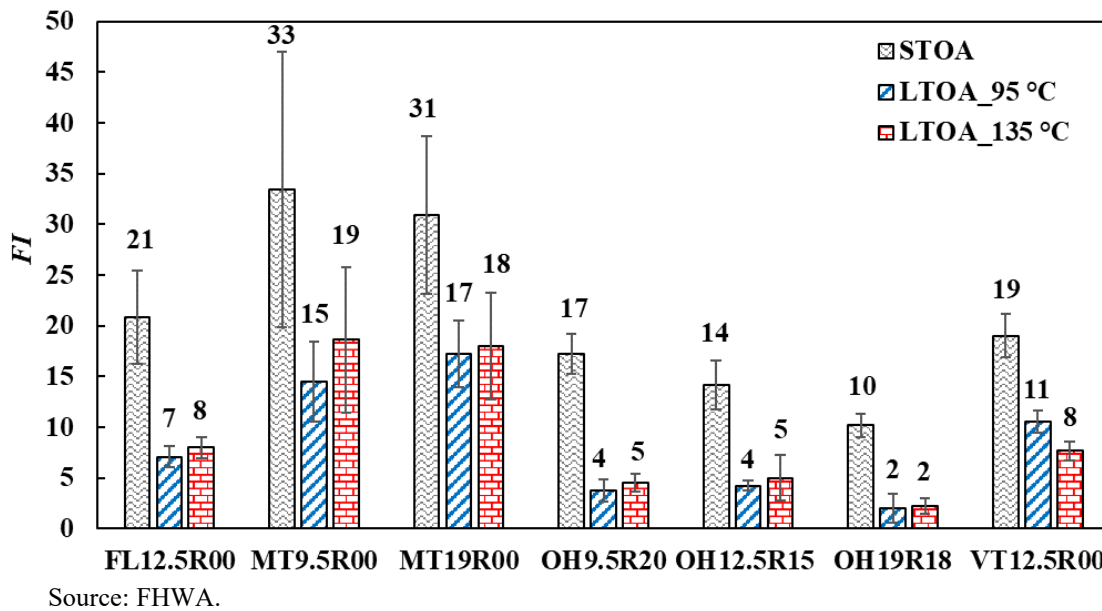


Figure 11. Graph. FI at STOA and LTOA levels for all mixtures at testing temperature.

S_{app} Results

S_{app} results from the AMPT cyclic fatigue test are shown in figure 12 for all seven mixtures from four different States under STOA and LTOA. S_{app} values are calculated at their respective testing temperatures. Figure 12 represents three replicates from the test at each aging level. S_{app} values show different trends compared with IDEAL-CT and I-FIT for a few mixtures. S_{app} value is higher during STOA; the value is reduced during LTOA except for Florida mixtures. After aging, the S_{app} value for Florida mixtures increased. For Montana 19-mm, Ohio 12.5-mm, and Vermont 12.5-mm, S_{app} at STOA shows similar values, but the index value dropped differently after aging.

Error bars in the figure represent the standard deviation of the replicates. Florida mixtures showed higher crack resistance compared with the other mixtures at all aging levels. The Ohio 19-mm mixture shows lower crack resistance at STOA. Ohio 9.5-mm shows lower cracking resistance under LTOA conditions. ANOVA shows a statistically significant difference between STOA and LTOA but not between the two LTOA methods.

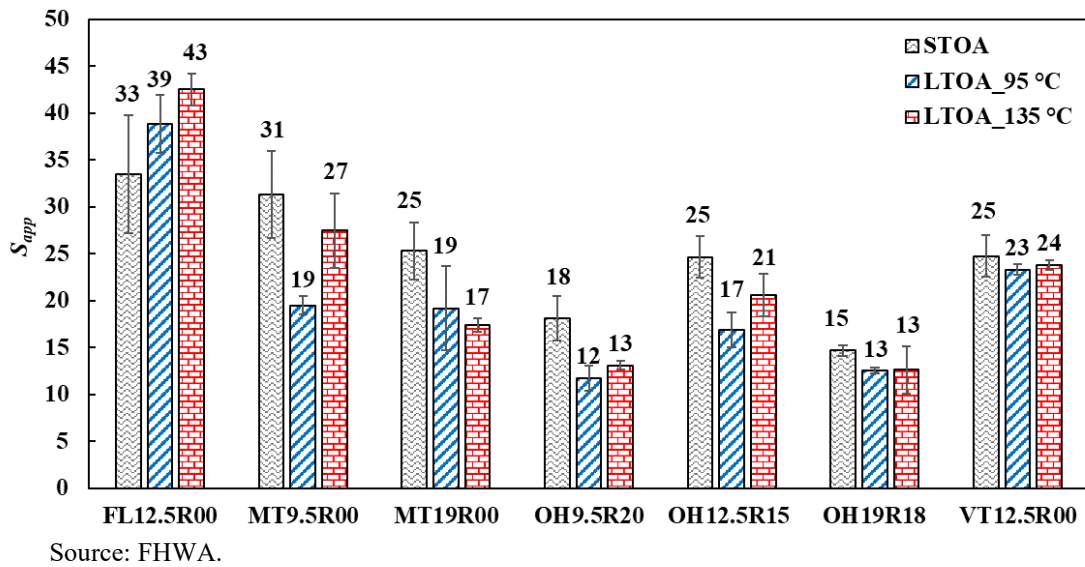


Figure 12. Graph. S_{app} at STOA and LTOA levels for all mixtures at individual testing temperature.

Figure 13 shows S_{app} index value results generated in the FlexMAT analysis workbook at 18 °C (64.4 °F) using the same data from the AMPT cyclic fatigue test at respective test temperatures. Because the IDEAL-CT and I-FIT were conducted at one temperature (25 °C (77 °F)), evaluating how the S_{app} index changes at one single temperature would be helpful. Figure 13 shows that the pattern does not change for most of the mixtures. The fatigue test temperature for Ohio mixtures was 18 °C (64.4 °F), so there is no change in value when compared with figure 12.

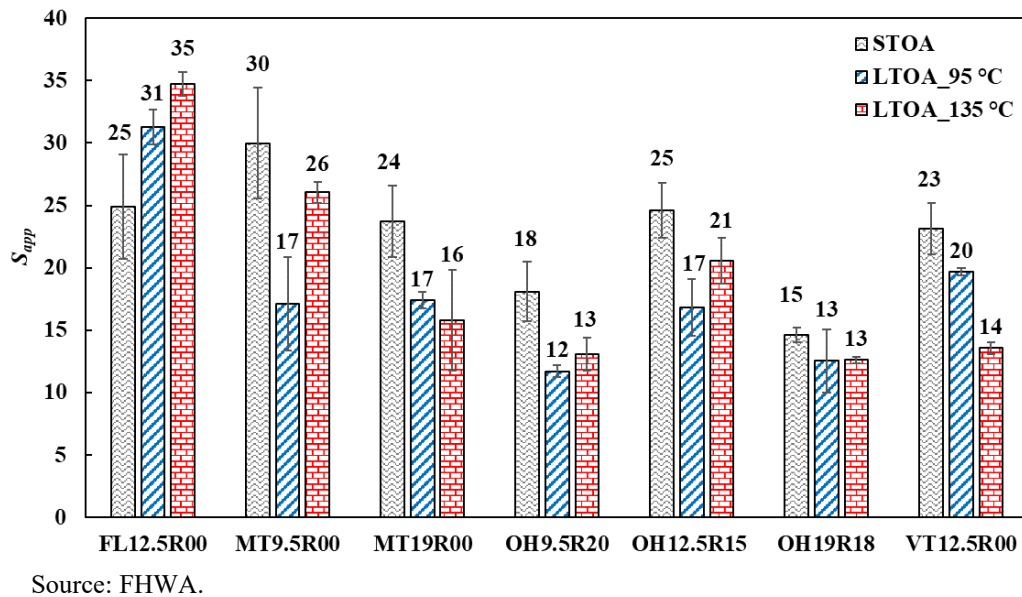
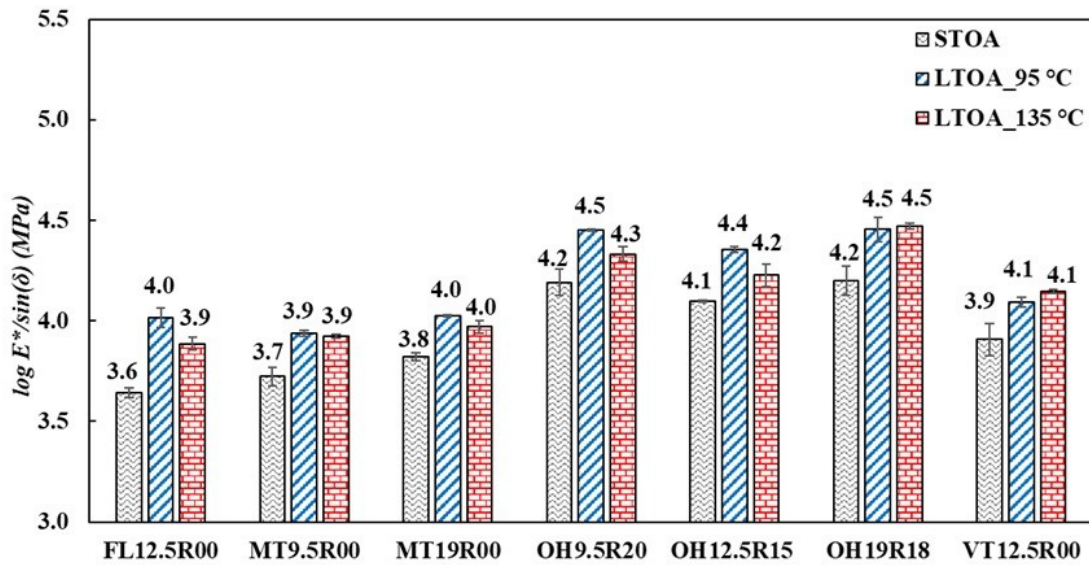


Figure 13. Graph. S_{app} at STOA and LTOA levels for all mixtures at 18 °C (64.4 °F).

$E^*/\sin(\delta)$ Results

Figure 14 shows results from $|E^*|/\sin(\delta)$, which this project used as an aging index, and that the $|E^*|/\sin(\delta)$ value is the same after the two LTOA conditioning methods except for a couple of mixtures. The results indicate that the possibility of change in RAP percentages drives the material's response. Student's t-test and ANOVA show a statistically significant difference between the two LTOA conditioning methods. STOA shows softer behavior than the two LTOA conditions, which matches the results from the first phases of this project.^(16,26)

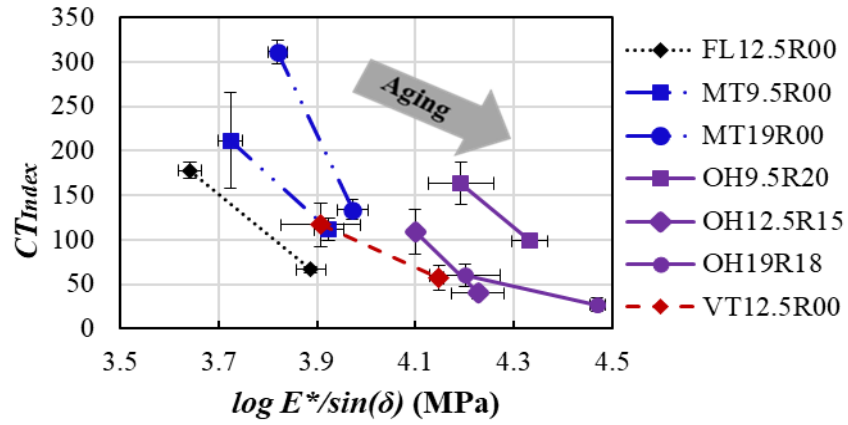


Source: FHWA.

Figure 14. Graph. Log $E^*/\sin(\delta)$ at STOA and LTOA levels for all mixtures at testing temperature.

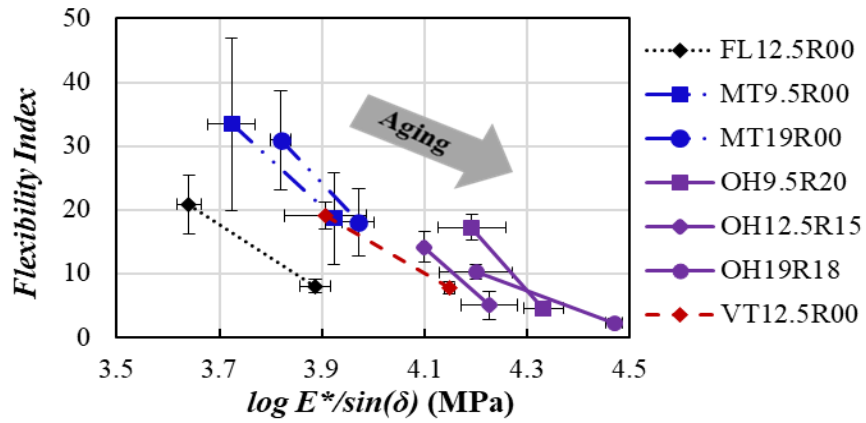
Mapping Linear Viscoelastic Aging Index Against Cracking Tests for STOA Versus LTOA

The commentary in this section pertains to figure 15 and figure 16, which show the linear viscoelastic index plotted against the three cracking test indexes. Each lane is represented on the plot by two points. In figure 15, the first point, with a smaller $|E^*|/\sin(\delta)$ value, represents the STOA condition; the second point, with a larger $|E^*|/\sin(\delta)$ value, represents the 135 °C (275 °F) LTOA procedure. In figure 16, the first point, with a smaller $|E^*|/\sin(\delta)$ value, represents the STOA condition; the second point, with a larger $|E^*|/\sin(\delta)$ value, represents the 95 °C (203 °F) LTOA procedure. The only parameter capable of showing universal agreement in trends from reheated to LTOA condition was $|E^*|/\sin(\delta)$, further proving that parameter's utility as an aging index. An arrow is drawn with the direction of expected progression for the indexes with increased aging. Error bars represent the standard deviation of replicates of their respective test methods. The figures show that all test indexes follow the same pattern from STOA to LTOA (reducing value) except for the Florida 12.5-mm mixture.



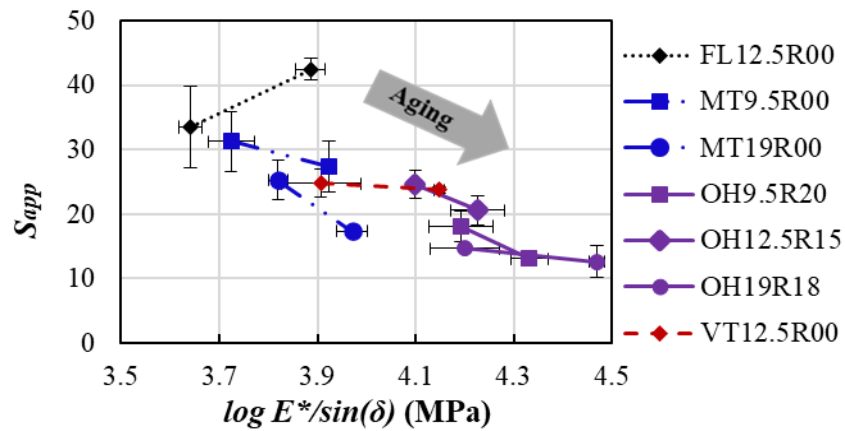
Source: FHWA.

A. CT_{Index} .



Source: FHWA.

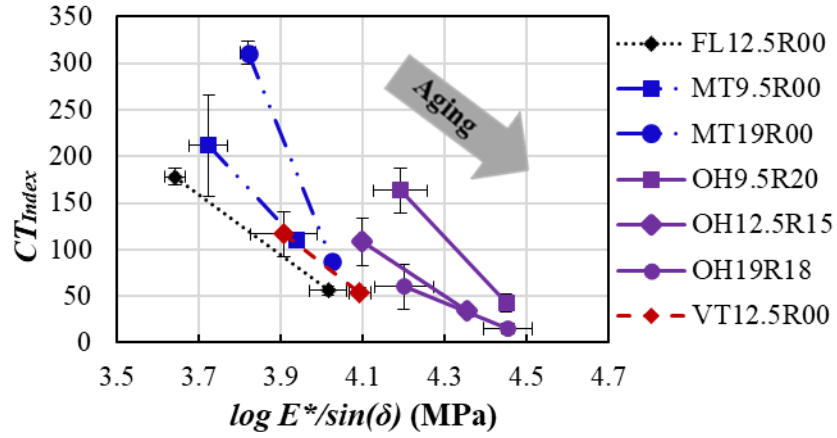
B. FI .



Source: FHWA.

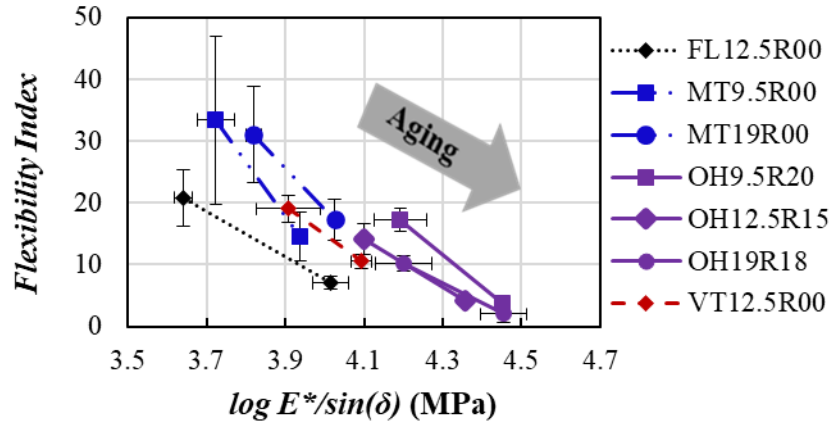
C. S_{app} .

Figure 15. Graphs. Relationship between cracking test indexes and $|E^*|/\sin(\delta)$ at STOA and 135 °C (275 °F) LTOA.



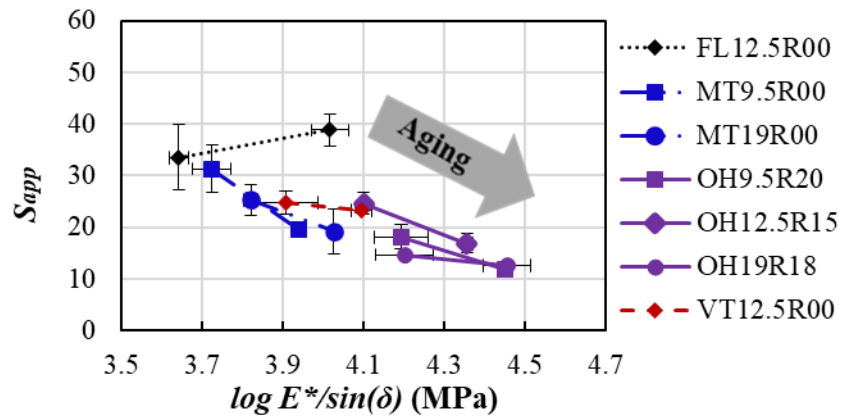
Source: FHWA.

A. CT_{Index} .



Source: FHWA.

B. FI .



Source: FHWA.

C. S_{app} .

Figure 16. Graphs. Relationship between cracking test indexes and $|E^*|/\sin(\delta)$ at STOA and 95 °C (203 °F) LTOA.

Table 3 summarizes all the index values at test temperatures, and table 4 summarizes COV values for each index value. As mentioned earlier in the *FI* results section, I-FIT displayed higher variability.

Table 3. Summary of index values from the four States at different aging levels.

Mixture ID	S_{app}	CT_{Index}	FI	$\text{Log } E^*/\text{Sin}(\delta)$
FL12.5R00	33.5	178	20.8	3.6
FL12.5R00 8H	42.5	67	8.0	3.9
FL12.5R00 7D	38.8	56	7.1	4.0
MT9.5R00	31.3	212	33.4	3.7
MT9.5R00 8H	27.5	112	18.6	3.9
MT9.5R00 3D	19.5	110	14.5	3.9
MT19R00	25.3	311	30.9	3.8
MT19R00 8H	17.4	134	18.0	4.0
MT19R00 3D	19.2	87	17.3	4.0
OH9.5R20	18.1	163	17.2	4.2
OH9.5R20 8H	13.1	99	4.5	4.3
OH9.5R20 4D	11.7	42	3.8	4.5
OH12.5R15	24.6	109	14.2	4.1
OH12.5R15 8H	20.6	40	5.0	4.2
OH12.5R15 4D	16.8	34	4.3	4.4
OH19R18	14.7	60	10.2	4.2
OH19R18 8H	12.6	27	2.3	4.5
OH19R18 4D	12.5	15	2.0	4.5
VT12.5R00	24.7	117	19.0	3.9
VT12.5R00 8H	23.8	57	7.7	4.1
VT12.5R00 3D	23.3	54	10.5	4.1

Table 4. Summary of COV (in percent) of index values from the four different States at different aging levels.

Mixture	S_{app}	CT_{Index}	FI
FL12.5R00	19	5	22
FL12.5R00 8H	4	5	13
FL12.5R00 7D	8	9	15
MT9.5R00	15	26	41
MT9.5R00 8H	14	11	38
MT9.5R00 3D	5	4	27
MT19R00	12	4	25
MT19R00 8H	4	8	29
MT19R00 3D	23	5	19
OH9.5R20	13	15	11
OH9.5R20 8H	4	5	20
OH9.5R20 4D	11	23	30
OH12.5R15	9	23	17
OH12.5R15 8H	11	15	44
OH12.5R15 4D	11	14	11
OH19R18	4	22	12
OH19R18 8H	20	28	33
OH19R18 4D	2	10	70
VT12.5R00	9	21	11
VT12.5R00 8H	2	23	12
VT12.5R00 3D	2	9	10

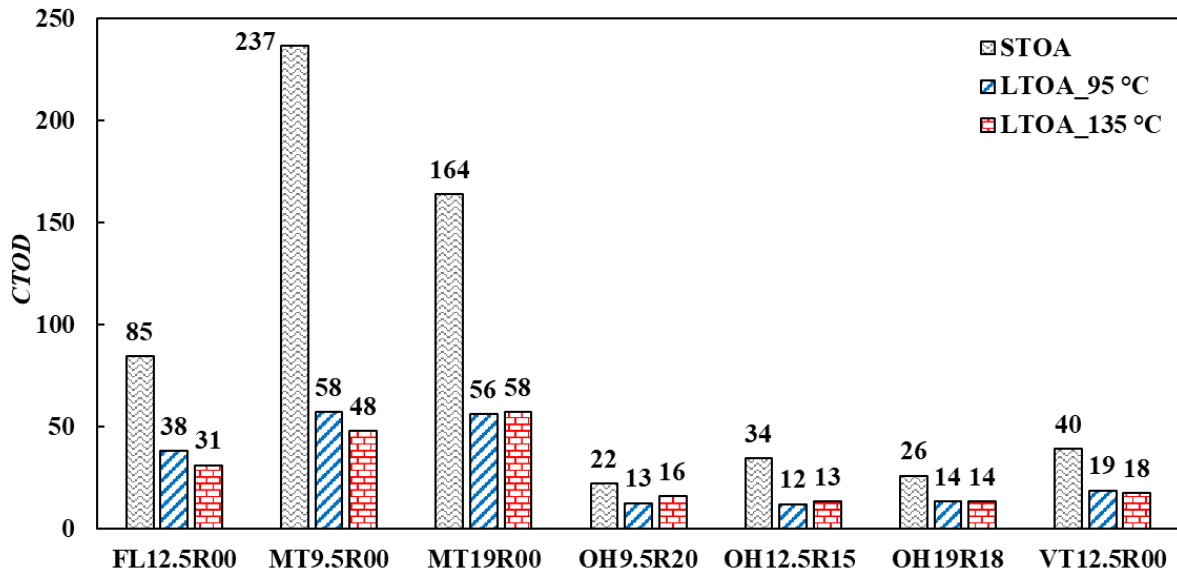
PHASE III BINDER RESULTS DISCUSSION

Binder strain tolerance (CTOD) is a parameter that, in the past, has correlated well with material fatigue resistance.^(44,45) A soft material has the advantage of absorbing a larger plastic deformation energy before a catastrophic failure, while the amount of energy involved in material separation can be pursued at lower strengths during larger deformation spans. From that perspective, the recovered binder from STOA with Florida 12.5-mm, Montana 9.5-mm, and Montana 19-mm may be considered top original performers. The mixture fracture performance testing at STOA aligns with the CTOD

results in the binder. Continuum damage S_{app} values fall short of that trend and are more in line with the rheological parameters of the mixtures or binders.

The strain tolerance also captures the dramatic effects of STOA and LTOA at various temperatures on the failure performance of all recovered binders. The original top performers (Florida 12.5 mm, Montana 9.5-mm, and Montana 19-mm) maintain the top positions. For these materials, the decrease in strain tolerance upon aging is three to four times compared with much more modest decreases for the rest of the materials. In addition, the CT_{Index} and FI parameter decrease between the STOA and LTOA conditions for these three materials is an impressive factor of two to three times. Such behavior in binder and mixture materials signals that binder aging characteristics can be successfully captured in the mixtures through fracture mechanics testing. In short, larger variations captured in binder testing with aging are also captured as characteristics of mixture testing.

The Ohio mixtures with 15-percent, 18-percent, and 20-percent RAP content exhibit distinct behavior during the aging process, as reflected in CTOD values, as they are described in figure 17. The long-term aging process leads to similar strain tolerance values for oven aging temperatures of 95 °C (203 °F) and 135 °C (275 °F), which may be the result of the high RAP content that can dampen the extent of strain tolerance loss during aging conditioning. Among the poorer performers, the Vermont material has a greater strain tolerance variation with aging, and the aging dampening effect of RAP is not manifesting in this case.



Source: FHWA.

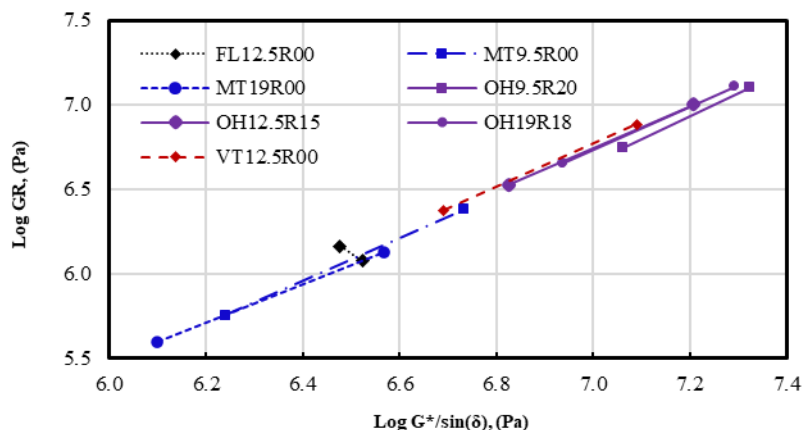
Figure 17. Graph. CTOD at STOA and LTOA levels for all mixtures.

Binder Rheology Correlations

The GR parameter was calculated from master curve data generated from DSR isotherms, shifted at 20 °C (68 °F). As expected, the rheological material parameters measured at similar strains and temperatures have a high degree of correlation. The GR values follow a trend similar to other rheological values, like the loss modulus. Figure 18 and figure 19 indicate that GR and the loss

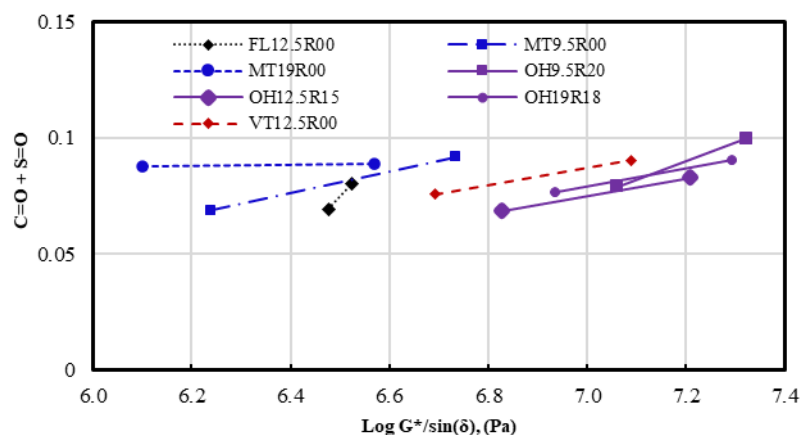
modulus are well correlated, and aging is producing similar magnitude increases in GR and loss modulus values. No clear correlation exists between the binder rheology and fracture mechanics parameters for the binder or the mix.

In addition, no apparent correlation exists between the chemical oxidation (carbonyl, C=O, and sulfoxide, S=O), functional groups, and rheological GR and loss modulus values, which may be a result of disruptive recovery conditions in which the trichloroethylene solvent may react with the functional groups of the recovered binders.



Source: FHWA.

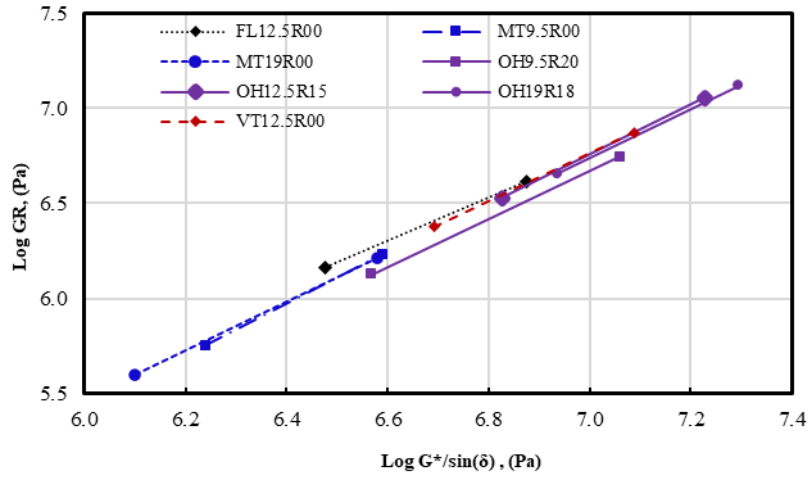
A. G_R .



Source: FHWA.

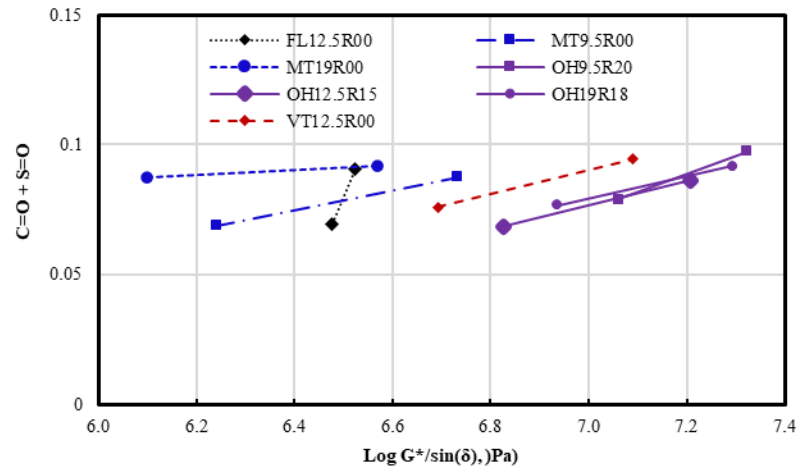
B. C=O + S=O at 135 °C (275 °F).

Figure 18. Graph. Relationship between cracking test indexes and $|G^*|/\sin(\delta)$ at STOA and 135 °C (275 °F) LTOA.



Source: FHWA.

A. G_R .



Source: FHWA.

B. $C=O + S=O$ at 95 °C (203 °F).

Figure 19. Graphs. Relationship between cracking test indexes and $|G^*|/\sin(\delta)$ at STOA and 95 °C (203 °F) LTOA.

CHAPTER 5. CONCLUSIONS

The aim of the study was to investigate the impacts of LTOA on mixture performance. In this study, mixtures from four different States with different RAP percents were studied both at STOA state and after two emerging LTOA conditioning methods to understand the diversity of the mixtures and stiffness dependency of the test methods. The researchers studied three intermediate cracking temperature indexes in the laboratory. The following remarks are based on results from the study:

- All three cracking test indices (S_{app} , FI , CT_{Index}) showed higher crack resistance indexes at STOA, and the value dropped during LTOA (95 °C and 135 °C (203 °F and 275 °F, respectively)).
- Results from IDEAL-CT show a clear difference between STOA and LTOA cracking performance; LTOA shows a sharp decrease in the cracking indices of those mixtures.
- I-FIT displayed higher variability than the other testing methods, which can be seen in the larger error bars in the figures.
- Results from this study match well with results from phase II of FHWA's study.⁽¹⁹⁾
- Cyclic fatigue test showed reasonable variability of test data and was successful in differentiating between aging levels.

ACKNOWLEDGMENTS

The authors thank Scott Parobeck, Frank Davis, and Bethel LaPlana of SES Group and Associates, LLC, for fabricating specimens and performing the testing required in this study. Technical input provided by Eshan Dave, Ph.D., of the University of New Hampshire; Andrew Hanz, Ph.D., of Mathy Construction; Nam Tran, Ph.D., of NCAT; Leslie McCarthy, Ph.D., of FHWA; Ross “Oak” Metcalfe of the Montana Department of Transportation; and Howie Moseley of the Florida Department of Transportation aided in the testing matrix formulation, and much gratitude is extended to each individual.

REFERENCES

1. Hubbard, P., and C. S. Reeve. 1913. "The Effect of Exposure on Bitumens." *Journal of Industrial and Engineering Chemistry* 5, no. 1: 15–18.
2. Thurston, R., and E. Knowles. 1936. "Oxygen Absorption Tests on Asphalt Constituents." *Journal of Industrial and Engineering Chemistry* 28, no. 1: 88–91.
3. Van Oort, W. P. 1956. "Durability of Asphalt—It's Aging in the Dark." *Journal of Industrial and Engineering Chemistry* 48, no. 7: 1196–1201.
<https://pubs.acs.org/doi/pdf/10.1021/ie50559a033>, last accessed February 5, 2024.
4. Corbett, L. W., and R. E. Merz. 1975. "Asphalt Binder Hardening in the Michigan Test Road After 18 Years of Service." *Transportation Research Record* 544: 27–34.
<https://trid.trb.org/view/35756>, last accessed February 5, 2024.
5. Kim, Y. R., C. Castorena, M. D. Elwardany, F. Y. Rad, S. Underwood, A. Gundla, P. Gudipudi, M. J. Farrar, and R. R. Glaser. 2018. NCHRP Report 871: *Long-Term Aging of Asphalt Mixtures for Performance Testing and Prediction*. Washington, DC: Transportation Research Board.
6. Elwardany, M. D., F. Yousefi Rad, C. Castorena, and Y. R. Kim. 2017. "Evaluation of Asphalt Mixture Laboratory Long-Term Ageing Methods for Performance Testing and Prediction." *Road Materials and Pavement Design* 18, Suppl 1: 28–61. <https://trid.trb.org/view/1448216>, last accessed February 5, 2024.
7. Partl, M. N., H. U. Bahia, F. Canestrari, C. De la Roche, H. Di Benedetto, H. Piber, and D. Sybilski. 2013. *Advances in Interlaboratory Testing and Evaluation of Bituminous Materials*. Champs-sur-Marne, France: International Union of Laboratories and Experts in Construction Materials, Systems and Structures.
8. Braham, A. F., W. G. Buttlar, T. R. Clyne, M. O. Marasteanu, and M. I. Turos. 2009. "The Effect of Long-Term Laboratory Aging on Asphalt Concrete Fracture Energy." *Journal of the Association of Asphalt Paving Technologies* 78.
9. Rad, F. Y., M. D. Elwardany, C. Castorena, and Y. R. Kim. 2017. "Investigation of Proper Long-Term Laboratory Aging Temperature for Performance Testing of Asphalt Concrete." *Construction and Building Materials* 147, 616–629.
10. AASHTO. 2019. *Standard Practice for Mixture Conditioning of Hot Mix Asphalt (HMA)*. AASHTO R 30. Washington, DC: American Association of State Highway and Transportation Officials.
11. National Academies of Sciences, Engineering, and Medicine. 2017. *Long-Term Aging of Asphalt Mixtures for Performance Testing and Prediction*. Washington, DC: The National Academies Press. <https://doi.org/10.17226/24959>, last accessed February 5, 2024.

12. Kim, Y. R., C. Castorena, M. Elwardany, F. Y. Rad, S. Underwood, G. Akshay, P. Gudipudi, M. J. Farrar, and R. R. Glasar. 2017. *Long-Term Aging of Asphalt Mixtures for Performance Testing and Prediction*. Report 871. Washington, DC: National Cooperative Highway Research Program.
13. Chen, C., F. Yin, P. Turner, R. C. West, and N. Tran. 2018. "Selecting a Laboratory Loose Mix Aging Protocol for the NCAT Top-Down Cracking Experiment." *Transportation Research Record* 2672, no. 28: 359–371.
14. AASHTO. 2019. *Standard Method of Test for Determining the Dynamic Modulus for Asphalt Mixtures Using Small Specimens in the Asphalt Mixture Performance Tester (AMPT)*. AASHTO TP 132. Washington, DC: American Association of State Highway and Transportation Officials.
15. Golalipour, A., V. Veginati, and D. J. Mensching. 2021. "Evaluation of Asphalt Mixture Performance Using Different Cracking and Durability Tests on Accelerated Pavement Test Sections." *Transportation Research Record* 2675, no. 11. <https://doi.org/10.1177/03611981211021856>, last accessed February 12, 2024.
16. Zhou, F., S. Im, L. Sun, and T. Scullion. 2017. "Development of an IDEAL Cracking Test for Asphalt Mix Design and QC/QA." *Road Materials and Pavement Design* 18: Suppl 4: 405–427.
17. ASTM. 2019. *Standard Test Method for Determination of Cracking Tolerance Index of Asphalt Mixture Using the Indirect Tensile Cracking Test at Intermediate Temperature*. ASTM D8225. West Conshohocken, PA: American Society for Testing and Materials.
18. Bahia, H., Y. Zhang, D. Swiertz, and A. Soleimanbeigi. 2020. *Long-Term Performance of Asphalt Concrete Mixed With RAP and RAS*. Final Report, Transportation Pooled Fund Study TPF-5(352). Madison, WI: Wisconsin Department of Transportation.
19. Mensching, D. J., M. D. Elwardany, and V. Veginati. 2022. "Evaluating the Sensitivity of Intermediate Temperature Performance Tests to Multiple Loose Mixture Aging Conditions Using the FHWA Accelerated Loading Facility's RAP/RAS Experiment." *Transportation Research Record* 2676, no. 10: 474–485. <https://doi.org/10.1177/03611981221090237>, last accessed February 5, 2024.
20. Al-Qadi, I. L., H. Ozer, J. Lambros, A. El Khatib, P. Singhvi, T. Khan, J. Rivera-Perez, and B. Doll. 2015. *Testing Protocols to Ensure Performance of High Asphalt Binder Replacement Mixes Using RAP and RAS*. Report No. FHWA-ICT-15-017. Urbana, IL: Illinois Center for Transportation.
21. Ozer, H., I. L. Al-Qadi, E. Barber, E. Okte, Z. Zhu, and S. Wu. 2017. *Evaluation of I-FIT Results and Machine Variability Using MNROAD Test Track Mixtures*. Report No. FHWA-ICT-17-012. Urbana, IL: Illinois Center for Transportation.

22. AASHTO. 2022. *Standard Method of Test for Determining the Fracture Potential of Asphalt Mixtures Using the Illinois Flexibility Index Test (I-FIT)*. AASHTO T 393. Washington, DC: American Association of State Highway and Transportation Officials.
23. Epps Martin, A., F. Kaseer, E. Arambula-Mercado, A. Bajaj, L. Garcia Cucalon, F. Yin, A. Chowdhury, et al. 2020. *Evaluating the Effects of Recycling Agents on Asphalt Mixtures With High RAS and RAP Binder Ratios*. Report 927. Washington, DC: National Cooperative Highway Research Program.
24. Ling, C., D. Swiertz, T. Mandal, P. Teymourpour, and H. Bahia. 2017. “Sensitivity of the Illinois Flexibility Index Test to Mixture Design Factors.” *Transportation Research Record* 2631: 153–159.
25. Witczak, M. W. 1999. *NCHRP 09-19: Superpave support and Performance Models Management*. Washington, DC: Transportation Research Board,.
<https://apps.trb.org/cmsfeed/TRBNetProjectDisplay.asp?ProjectID=955>.
26. Bonaquist, R. 2008. *NCHRP Report 629: Ruggedness Testing of the Dynamic Modulus and Flow Number Tests with the Simple Performance Tester*. Transportation Research Board, Washington, DC, p. 39. <https://doi.org/10.17226/14200>, last accessed June 17, 2024.
27. AASHTO. 2015. *Standard Method of Test for Determining the Dynamic Modulus and Flow Number for Asphalt Mixtures Using the Asphalt Mixture Performance Tester (AMPT)*. AASHTO TP 79. Washington, DC: American Association of State Highway and Transportation Officials.
28. Witczak, M. W. 2005. Simple Performance Tests: Summary of Recommended Methods and Database. *National Cooperative Highway Research Program*. Report 547. Washington, DC: Transportation Research Board.
29. Mensching, D. J., G. M. Rowe, J. S. Daniel, and T. Bennert. 2015. “Exploring Low Temperature Performance in Black Space.” *Journal of Road Materials and Pavement Design* 16, Special Issue: *90th Association of Asphalt Paving Technologists Annual Meeting*. Portland, OR. <https://doi.org/10.1080/14680629.2015.1077015>, last accessed February 12, 2024.
30. Mensching D. J., G. M. Rowe, and J. S. Daniel. 2016. “Mixture-1 Based Black Space Parameter for Low Temperature Performance of Hot Mix Asphalt.” *Journal of Road Materials and Pavement Design* 17, Special Issue: *91st Association of Asphalt Paving Technologists Annual Meeting*. Indianapolis, IN. <https://doi.org/10.1080/14680629.2016.1266770>, last accessed February 12, 2024.
31. Wang, Y. D., B. S. Underwood, and Y. R. Kim. 2020. “Development of a Fatigue Index Parameter, S_{app} , for Asphalt Mixes Using Viscoelastic Continuum Damage Theory.” *International Journal of Pavement Engineering* 23, no. 2: 438–452.
<https://doi.org/10.1080/10298436.2020.1751844>, last accessed February 13, 2024.

32. FHWA. 2019. *Cyclic Fatigue Index Parameter (S_{app}) for Asphalt Performance Engineered Mixture Design*. Publication No. FHWA-HIF-19-091. Washington, DC: Federal Highway Administration.
33. AASHTO. 2023. *Standard Method of Test for Determining the Damage Characteristic Curve of Asphalt Mixtures from Direct Tension Cyclic Fatigue Tests*. AASHTO T 411. Washington, DC: American Association of State Highway and Transportation Officials.
34. Kim, Y. R., C. Castorena, N. F. Saleh, E. Braswell, M. Elwardany, and F. Y. Rad. 2020. *NCHRP 09-54 Extension Report: Long-Term Aging of Asphalt Mixtures for Performance Testing and Prediction*. Washington, DC: Transportation Research Board.
<https://doi.org/10.17226/26133>, last accessed February 5, 2024.
35. Saleh, N. F., B. Keshavarzi, F. Y. Rad, D. Mocelin, M. Elwardany, C. Castorena, B. S. Underwood, and Y. R. Kim. 2020. "Effects of Aging on Asphalt Mixture and Pavement Performance." *Construction and Building Materials* 258: 120309.
36. ASTM. 2017. *Standard Test Methods for Quantitative Extraction of Bitumen From Bituminous Paving Mixtures*. ASTM D2172. West Conshohocken, PA: ASTM International.
37. ASTM. 2003. *Standard Practice for Recovery of Asphalt from Solution Using the Rotary Evaporator*. ASTM D5404. West Conshohocken, PA: ASTM International.
38. AASTHO. 2010. *Determining the Rheological Properties of Asphalt Binder Using a Dynamic Shear Rheometer (DSR)*. AASHTO T 315. Washington, DC: American Association of State Highway and Transportation Officials.
39. Marasteanu, M. O., and D. A. Anderson. 1999. "Improved Model for Bitumen Rheological Characterization." Presented at *Eurobitume Workshop on Performance Related Properties for Bituminous Binders 133*. Brussels, Belgium: European Bitumen Association.
40. Rowe, G. M. 2011. Prepared Discussion for the AAPT paper by Anderson et al.: Evaluation of the Relationship Between Asphalt Binder Properties and Non-Load Related Cracking. *Journal of the Association of Asphalt Paving Technologists* 80: 649–662.
41. AASHTO. 2023. *Standard Method of Test for Determination of Asphalt Binder Resistance to Ductile Failure Using Double-Edge-Notched Tension (DENT) Test*. AASHTO T 405. Washington, DC: American Association of State Highway and Transportation Officials.
42. Cotterell, B., and J. K. Reddel. 1977. "The Essential Work of Plane Stress Ductile Fracture." *International Journal of Fracture* 13, no. 3: 267–277.
43. Petersen, J. C. 2009. "A Review of the Fundamentals of Asphalt Oxidation: Chemical, Physicochemical, Physical Property, and Durability Relationships." *TRB Transportation Research Circular E-C140*.
44. Andriescu, A., S. A. M. Hesp, and J. S. Youtcheff. 2004. "Essential and Plastic Works of Ductile Fracture in Asphalt Binders." *Transportation Research Record* 1875: 1–8.

45. Andriescu, A., N. Gibson, S. A. M. Hesp, X. Qi, and J. Youtcheff. 2006. "Validation of the Essential Work of Fracture Approach to Fatigue Grading of Asphalt Binders." *Journal of the Association of Asphalt Paving Technologists* 75E: 1–37.



Recycled
Recyclable

Recommended citation: Federal Highway Administration,
*Evaluating the Sensitivity of Intermediate Temperature
Performance Tests With Short-Term and Long-Term Laboratory
Conditioning: Validation Study* (Washington, DC: 2024)
<https://doi.org/10.21949/1521783>

HRDI-10/01-25(WEB)E